Anal. Chem. **1995**, *67*, 196–207

Electrospray Ionization Mass Spectrometry of Sphinganine Analog Mycotoxins

Eloisa D. Caldas,[†] A. Daniel Jones,*[,‡] Carl K. Winter,[†] Barney Ward,[§] and David G. Gilchrist[§]

Department of Food Science and Technology, Facility for Advanced Instrumentation, and Department of Plant Pathology, University of California, Davis, California 95616

The ionization and fragmentation behavior of two groups of sphinganine analog mycotoxins (SAMs), the AAL toxins (TA, TB, TC, TD, and TE) and fumonisins (FB_1 and FB_2), were compared in positive and negative electrospray ionization (ESI) modes. Toxins containing amino groups yielded abundant $[M + H]^+$ in positive mode, whereas N-acetylated toxin congeners were protonated less efficiently but yielded abundant $[M + Na]^+$ ions. Negative ESI mass spectra exhibited abundant $[M - H]^-$ ions for all toxins, and fumonisins could be distinguished by the presence of additional peaks corresponding to $[M - 2H]^{2-}$. Negative mode ionization facilitated the detection of a new AAL toxin, corresponding to N-acetylated TA, that was not evident in positive ESI mass spectra of a fungal culture filtrate. Low-energy collisional activation of deprotonated toxins yielded fragment ions characteristic of the tricarballylic acid moiety, whereas protonated toxins fragmented to give more information about the structure of the rest of the molecule. Collisional activation performed in the transport region of the electrospray source yielded fragment patterns similar to those obtained from low-energy collision activated dissociation generated in a collision cell. AAL toxins TA and TD were detected in spiked extracts of vegetable juice and fumonisin FB was detected in spiked corn extracts using positive ESI, with detection limits ranging from 4 to 10 μg/mL injected. Additional sample cleanup will be required for confirmation of SAM contamination of foods at sub-parts per million levels using flow injection ESI since unidentified matrix components suppressed ionization in both positive and negative modes. At present, ESI in positive or negative mode is the only analytical tool shown to be capable of detecting all SAM congeners.

AAL toxins and fumonisins are two groups of mycotoxins that bear structural similarities and exhibit similar toxicological properties. They are produced respectively by the fungi *Alternaria alternata* f.sp. *lycopersici* and *Fusarium moniliforme*, both of which are commonly found on various food crops.[1-3] These two groups of toxins can be classified as sphinganine analog mycotoxins (SAMs) due to their structural similarity to the backbone structure of sphingolipids. AAL toxins consist of a long-chain aminopolyol backbone containing a tricarballylic ester group in either the C_{13} or C_{14} position,[4-6] while the fumonisins are bistricarballylic esters of similar aminopolyols (Figure 1).[7]

Both AAL toxins and fumonisins exhibit phytotoxic properties against a wide variety of weed and crop cultivars.[8,9] The most abundant of the fumonisin congeners, FB_1, exhibits toxicity in animals,[10-12] while human consumption of corn contaminated with FB_1 has been associated with esophageal cancer, although a causal linkage to the latter has not been established.[13] The widespread occurrence of FB_1 in corn at parts per million levels has led to a growing recognition of the need to determine levels of these toxins in foods consumed by humans and livestock. The AAL toxin TA exhibited toxicity to cultured mammalian cells[14] and, like FB_1, is reported to inhibit ceramide synthase.[15]

Various techniques have been employed for determination of SAMs, including HPLC[16,17] and immunoassay,[18] but additional toxins of this class continue to be discovered. The most commonly used HPLC methods rely upon the conversion of the amino group to fluorescent derivatives and fail to detect N-acetylated AAL toxins and fumonisins which have been observed in earlier studies.[6,19] Immunoassays provide aggregate toxin concentrations but provide little information about the amounts of individual SAM congeners. Assessments of toxicological properties and health risks posed by SAM congeners as well as detailed investigations into SAM biosynthesis require definitive methods for screening and structural confirmation that can provide information about the occurrence of all potentially toxic SAMs.

[†] Department of Food Science and Technology.
[‡] Facility for Advanced Instrumentation, 9 Hutchison Hall.
[§] Department of Plant Pathology.

(1) Gilchrist, D. G.; Grogan, R. G. *Phytopathology* **1976**, *66*, 165–171.
(2) Sydenham, E. W.; Marasas, W. F. O.; Shephard, G. S.; Thiel, P. G.; Hirooka, E. Y. *J. Agric. Food Chem.* **1992**, *40*, 994–997.
(3) Abbas, H. K.; Vesonder, R. F.; Boyette, C. D.; Hoagland, R. E.; Krick, T. J. *Phytopathology* **1992**, *136*, 119–203.
(4) Bottini, A. T.; Gilchrist, D. G. *Tetrahedron Lett.* **1981**, *22*, 2719–2722.
(5) Bottini, A. T.; Bowen, J. R.; Gilchrist, D. G. *Tetrahedron Lett.* **1981**, *22*, 2723–2726.
(6) Caldas, E. D.; Jones, A. D.; Ward, B.; Winter, C. K.; Gilchrist, D. G. *J. Agric. Food Chem.* **1994**, *42*, 327–333.
(7) Bezuidenhout, S. C.; Gelderblom, W. C. A.; Gorst-Allman, C. P.; Horak, R. M.; Marasas, W. F. O.; Spiteller, G.; Vleggaar, R. *J. Chem. Soc., Chem. Commun.* **1988**, 743–745.
(8) Lamprecht, S. C.; Marasas, W. F. O.; Alberts, J. F.; Cawood, M. E.; Gelderblom, W. C. A.; Shephard, G. S.; Thiel, P. G.; Calitz, F. J. *Phytopathology* **1994**, *84*, 383–391.
(9) Gilchrist, D. G.; Ward, B.; Moussatos, V.; Mirocha, C. J. *Mycopathologia* **1992**, *117*, 57–64.
(10) Marasas, W. F. O.; Kellerman, T. S.; Gelderblom, W. C. A.; Coetzer, J. A. W.; Thiel, P. G.; van der Lugt, J. J. *Onderstepoort J. Vet. Res.* **1988**, *55*, 197–203.
(11) Voss, K. A.; Norred, W. P.; Plattner, R. D.; Bacon, C. W. *Food Chem. Toxicol.* **1989**, *27*, 89–96.
(12) Casteel, S. W.; Turk, J. R.; Cowart, R. P.; Rottinghaus, G. E. *J. Vet. Diag. Invest.* **1993**, *5*, 413–417.
(13) Marasas, W. F. O.; Jaskiewicz, K.; Venter, F. S.; van Schalkwyk, D. J. *S. Afr. Med. J.* **1988**, *74*, 110–114.
(14) Shier, W. T.; Abbas, H. K.; Mirocha, C. J. *Mycopathologia* **1991**, *116*, 97–104.
(15) Merrill, A. H., Jr.; Wang, E.; Gilchrist, D. G.; Riley, R. T. *Adv. Lipid Res.* **1993**, *26*, 215–234.
(16) Siler, D. J.; Gilchrist, D. G. *Physiol. Plant Pathol.* **1983**, *23*, 265–274.
(17) Thiel, P. G.; Sydenham, E. W.; Shephard, G. S.; van Schalkwyk, D. J. *J. Assoc. Off. Anal. Chem.* **1993**, *76*, 361–366.
(18) Azcona-Olivera, J. I.; Abouzied, M. M.; Plattner, R. D.; Norred, W. P.; Pestka, J. J. *Appl. Environ. Microbiol.* **1992**, *58*, 169–173.
(19) Cawood, M. E.; Gelderblom, W. C. A.; Vleggaar, R.; Behrend, Y.; Thiel, P. G.; Marasas, W. F. O. *J. Agric. Food. Chem.* **1991**, *39*, 1958–1962.

0003-2700/95/0367-0196$9.00/0

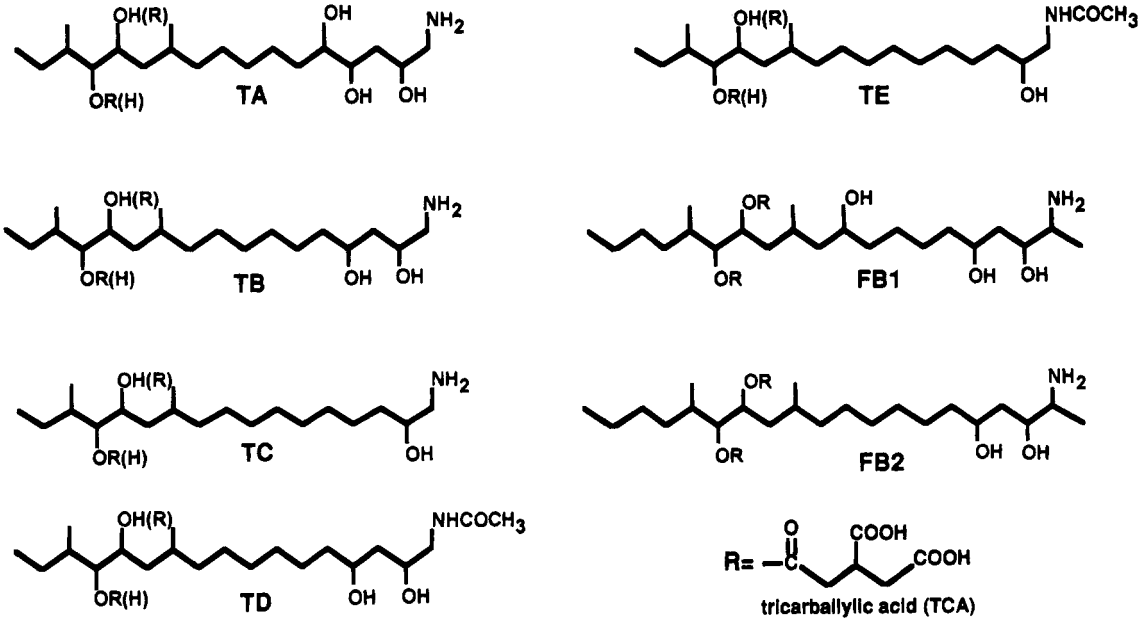

Figure 1. Structures of the AAL toxins and fumonisins.

A range of mass spectrometric ionization methods have been explored for detection of SAMs, including GC/MS,[20] LSIMS,[7,21] ion spray,[22] FAB,[23,24] particle beam under CI and EI conditions,[25] and electrospray ionization (ESI).[23] Though applications of ESI mass spectrometry have largely focused on characterization of large molecules such as proteins,[26–28] applications of ESI for analysis of smaller molecules, while promising, have yet to be extensively exploited.[29–31]

Most ESI mass spectrometry applications have been conducted in positive ion mode, which involves protonation at a basic functional group in a molecule. This mode has been especially useful for characterization of proteins and peptides that contain an abundance of such groups.[32] Conversely, negative ion mode ESI, which has often been ignored, results in deprotonation of acidic functional groups and is particularly suited to the analysis of acidic substances.[33,34] Since SAMs contain at least two carboxylic acid groups and a nitrogen that exists either as an amide or as a primary amine, both positive and negative modes are applicable for analysis of these compounds.

ESI is a gentle process in which $[M + H]^+$ is usually the predominant ion formed from small molecules in the positive ionization mode, and limited fragmentation is observed. However, formation of fragment ions via collision activated dissociation (CAD) has been used for structural characterization of proteins and polypeptides,[35,36] pesticides and antibiotics,[37] nucleotides and explosives.[33] Collisional activation can be induced in the electrospray transport region by varying the orifice potential or, in the case of tandem mass spectrometers, in a collision cell following a mass analyzer which allows for selection of ions of a chosen mass/charge ratio.

A goal of our current efforts is to determine the most appropriate mass spectrometric methods for screening and confirmation of all known SAMs in complex organic matrices, including plant material and fungal cultures. An additional goal has been to develop analytical techniques that would allow for recognition of the presence of heretofore unknown but structurally related mycotoxins. In the current work, we compare the ionization behavior of all five known AAL toxins and of two fumonisins, FB_1 and FB_2, in both positive and negative modes of ESI and provide evidence for the presence of a previously undetected AAL toxin congener. The usefulness of CAD in both the transport region and the collision cell is also described. Limitations to the use of flow injection ESI for rapid detection of FB_1 in field corn and AAL toxins TA and TD in vegetable juice are discussed.

EXPERIMENTAL SECTION

Reagents. Tricarballylic acid (TCA), β-methyltricarballylic acid, and FB_1 were obtained from Sigma Chemical Co. (St. Louis,

(20) Plattner, R. D.; Branham, B. E. *J. Assoc. Off. Anal. Chem.* **1994**, *77*, 525–532.
(21) Plattner, R. D.; Norred, W. P.; Bacon, C. W.; Voss, K. A.; Peterson, R.; Shackelford, D. D.; Weisleder, D. *Mycologia* **1990**, *82*, 698–702.
(22) Chen, J.; Mirocha, C. J.; Xie, W.; Hogge, L.; Olson, D. *Appl. Environ. Microbiol.* **1992**, *58*, 3928–3931.
(23) Korfmacher, W. A.; Chiarelli, M. P.; Lay, J. O., Jr.; Bloom, J.; Holcomb, M. *Rapid Commun. Mass Spectrom.* **1991**, *5*, 463–468.
(24) Holcomb, M.; Sutherland, J. B.; Chiarelli, M. P.; Korfmacher, W. A.; Thompson, H. C.; Lay, J. O., Jr.; Hankins, L. J.; Cerniglia, C. E. *J. Agric. Food Chem.* **1993**, *41*, 357–360.
(25) Young, J. C.; Lafontaine, P. *Rapid Commun. Mass Spectrom.* **1993**, *7*, 352–359.
(26) Smith, R. D.; Loo, J. A.; Edmonds, C. G.; Barinaga, C. J.; Udseth, H. R. *Anal. Chem.* **1990**, *62*, 882–899.
(27) Springer, D. L.; Bull, R. I.; Goheen, S. C.; Sylvester, D. M.; Edmonds, C. G. *J. Toxicol. Environ. Health* **1993**, *40*, 161–176.
(28) Huang, E. C.; Pramanik, B. N.; Tsarbopoulos, A.; Reichert, P.; Ganguly, A. K.; Trotta, P. P.; Nagabhushan, T. L.; Covey, T. R. *J. Am. Soc. Mass Spectrom.* **1993**, *4*, 624–630.
(29) Poon, G. K.; Bisset, G. M. F.; Mistry, P. *J. Am. Soc. Mass Spectrom.* **1993**, *4*, 588–595.
(30) Reiser, R. W.; Fogiel, A. J. *Rapid Commun. Mass Spectrom.* **1994**, *8*, 252–257.
(31) Poon, G. K.; Griggs, L. J.; Edwards, C.; Beattie, K. A.; Codd, G. A. *J. Chromatogr.* **1993**, *628*, 215–233.
(32) Smith, R. D.; Loo, J. A.; Ogorzalek Loo, R. R.; Busman, M.; Udseth, H. R. *Mass Spectrom. Rev.* **1991**, *10*, 359–451.
(33) Straub, R. F.; Voyskner, R. D. *J. Am. Soc. Mass Spectrom.* **1993**, *4*, 578–587.
(34) Rashed, M. S.; Ozand, P. T.; Harrison, M. E.; Watkins, P. J. F.; Evans, S. *Rapid Commun. Mass Spectrom.* **1994**, *8*, 129–133.
(35) Smith, R. D.; Loo, J. A.; Barinaga, C. J.; Edmonds, C. G.; Udseth, H. R. *J. Am. Soc. Mass Spectrom.* **1990**, *1*, 53–65.
(36) Fabris, D.; Kelly, M.; Murphy, C.; Wu, Z.; Fenselau, C. *J. Am. Soc. Mass Spectrom.* **1993**, *4*, 652–661.
(37) Voyksner, R. D.; Pack, T. *Rapid Commun. Mass Spectrom.* **1991**, *5*, 263–268.

MO). Positive mode ESI spectra of FB_1 indicated a purity greater than 95%. FB_2 was a gift from Chester J. Mirocha (University of Minnesota, St. Paul, MN) and was used without further treatment. Formic acid (FA), acetic acid, and ammonium hydroxide were purchased from Fisher Biotech (Fisher Scientific, Fair Lawn, NJ). Trifluoroacetic acid (TFA) and methyl-d_3 alcohol-d (99.8% D) were purchased from Aldrich Chemical Co. (Milwaukee, WI). The solvents used were HPLC grade (Fisher). Strong anion-exchange (SAX) and C_{18} solid phase extraction cartridges were purchased from Varian Associates (Harbor City, CA). Amberlite XAD-2 was purchased from Sigma and silica gel from Selecto Scientific (Kennesaw, GA). Vegetable juice (V8 juice) was obtained from a local market.

Toxin Preparations. AAL toxins were obtained from liquid cultures of *A. alternata* f.sp. *lycopersici* grown on standard media[38] modified by substitution of pectin for glucose (6 g/L). The culture was harvested, filtered, and extracted with Amberlite XAD-2 followed by SAX and flash chromatography, according to Caldas et al.[6] for the study of CAD in the transport region. The concentrations of the AAL toxins in prepared solutions were estimated on the basis of comparisons of the combined yields of $[M + H]^+$ (and $[M + Na]^+$ for acetylated toxins) using electrospray ionization in positive mode to the yield of $[M + H]^+$ obtained for a known amount of added FB_1, with no correction for mass discrimination.

Milligram quantities of AAL toxin standards for analysis in food matrices were prepared by processing five batches of *A. alternata* f.sp. *lycopersici* liquid culture as described by Caldas et al.[6] Following flash chromatography, the toxins were purified by HPLC (Beckman System Gold, Beckman Instruments, Inc., San Ramon, CA) at 210 nm using a reverse-phase C18 column (Ultracarb 7 ODS (30), 250 × 10.0 mm, Phenomenex, Rancho Palos Verdes, CA), using gradients of acetonitrile/water (containing 0.1% TFA) optimized separately for each toxin. The solvent was removed from the toxins under vacuum, the residues were weighed, and solutions of known concentration were prepared for use in the vegetable juice study. The purities of the HPLC-derived standards were determined to be greater than 95% on the basis of ESI mass spectra and ^1H NMR spectra.

Spectroscopic Analysis. All electrospray spectra were acquired using a VG Quattro-BQ triple quadrupole mass spectrometer (VG Biotech, Altrincham, U.K.), connected to a microflow pump (μLC-500, Isco, Inc., Lincoln, NE). The flow rate was held constant at 10 μL/min. Loop injections of 10 μL were made using a solvent system of CH_3OH:H_2O:FA (50:50:1) or 100% CH_3OH for positive ionization and 100% CH_3OH for negative ionization. The transport region temperature was maintained at 80 °C, and the capillary voltage was adjusted to give optimum ion yield at about 3.0 kV. The resolution of the mass analyzer was adjusted to give a peak width at half-height of about 2 Da/e for protonated FB_1. For tandem mass spectrometry experiments, argon was used as collision gas at a recorded pressure of 1.3×10^{-3} mBar. In the positive mode, mass calibration was performed using a solution of mixtures of poly(ethylene glycols) (300 pmol/μL). In the negative mode, mass calibration was performed using a mixture of sugars (60 nmol/μL). Selected ion monitoring (SIM) experiments in positive mode were performed using 522.3, 548.3, and 722.3 Da/e for TA, TD, and FB_1, respectively, and in negative mode using 520.3 and 546.3 Da/e for TA and TD, respectively. Dwell time was 0.2 s, and interchannel delay was 0.02 s. Full scan spectra were acquired using MCA mode spectrum summation over the range of 300–800 Da/e.

NMR spectra were obtained using a GE Ω-500 spectrometer (General Electric, Fremont, CA) at 500.136 MHz using a 5 mm probe at room temperature. Chemical shifts are reported on the basis of the chemical shift of the residual solvent CD_3OD peak (3.3 ppm). A correlated spectroscopy (COSY) experiment was performed with 128 scans each of 128 T_1 blocks each and size 1 kb.

Food Matrix: Corn. A 20 mL aliquot of water was added to a 20 g sample of ground field corn (Pioneer hybrid 3162), and the corn was soaked for 1 h and processed according to procedures described by Thiel et al.[17] Briefly, the sample was extracted in 75% CH_3OH and centrifuged, and two 5 mL aliquots of the supernatant were added to a 3 mL SAX column and eluted as described before.[17] The volume of the eluate was adjusted so that 1 mL of methanolic extract corresponded to 0.5 g of corn. Standard FB_1 was added to give final concentrations in the corn extract corresponding to a range from 2 ng to 20 μg of FB_1/g corn (1 ng/mL to 10 μg/mL solution). All samples were analyzed in positive ESI, in both MCA (full spectrum) and SIM acquisition modes. The concentration of FB_1 in an unspiked corn sample was below detectable limits.

Food Matrix: Vegetable Juice. Vegetable juice (100 mL) was centrifuged for 10 min at 10 000 rpm, the supernatant filtered through Whatman No. 1 filter paper, and the pH adjusted to 3.0 with acetic acid. Two separate 5 mL aliquots of the filtered supernatant were loaded onto 3 mL C18 cartridges preconditioned with 3 mL of 100% CH_3OH and equilibrated with 3 mL of water. The column was washed with 3 mL of water, followed by 5 mL of 40% CH_3OH, and then eluted with 8 mL of 90% CH_3OH. The eluate was adjusted to pH 8.0 with NH_4OH, and the solution was loaded onto a 3 mL SAX cartridge and eluted as described before.[17] The vegetable juice extracts were adjusted to a 1:1 ratio (extract volume:juice volume) with CH_3OH and spiked with TA and TD standards, giving equivalent concentrations of 2 ng to 20 μg of toxin/mL juice. Standard solutions of TA and TD were also prepared in CH_3OH at the same concentration, and the samples were analyzed by positive and negative ESI, using both MCA and SIM modes. Toxins were not present in detectable concentrations in unspiked vegetable juice.

RESULTS AND DISCUSSION

Positive and Negative ESI. A positive mode ESI spectrum of extracts from *A. alternata* f.sp. *lycopersici* liquid cultures revealed a set of peaks where each peak corresponded to a pair of protonated AAL toxin regioisomers consisting of an aminopolyol backbone with a tricarballylic ester attached at either C_{13} or C_{14} (Figure 2a). The $[M + H]^+$ ions at 522, 506, 490, 548, and 532 Da/e correspond to AAL toxins previously designated TA, TB, TC, TD, and TE, respectively.[6] For the congeners containing a free amino group (TA, TB, TC), cationization via sodium ion attachment generated minor peaks relative to $[M + H]^+$. However, sodium attachment represented a major ionization event for each of the acetylated congeners (TD at 570 Da/e, TE at 554 Da/e), which have lower proton affinities than their corresponding nonacetylated congeners. Positive mode spectra of the fumonisins FB_1 and FB_2 showed abundant $[M + H]^+$ peaks at 722 and 706

(38) Clouse, S. D.; Martensen, A. N.; Gilchrist, D. G. *J. Chromatogr.* **1985**, *350*, 255–263.

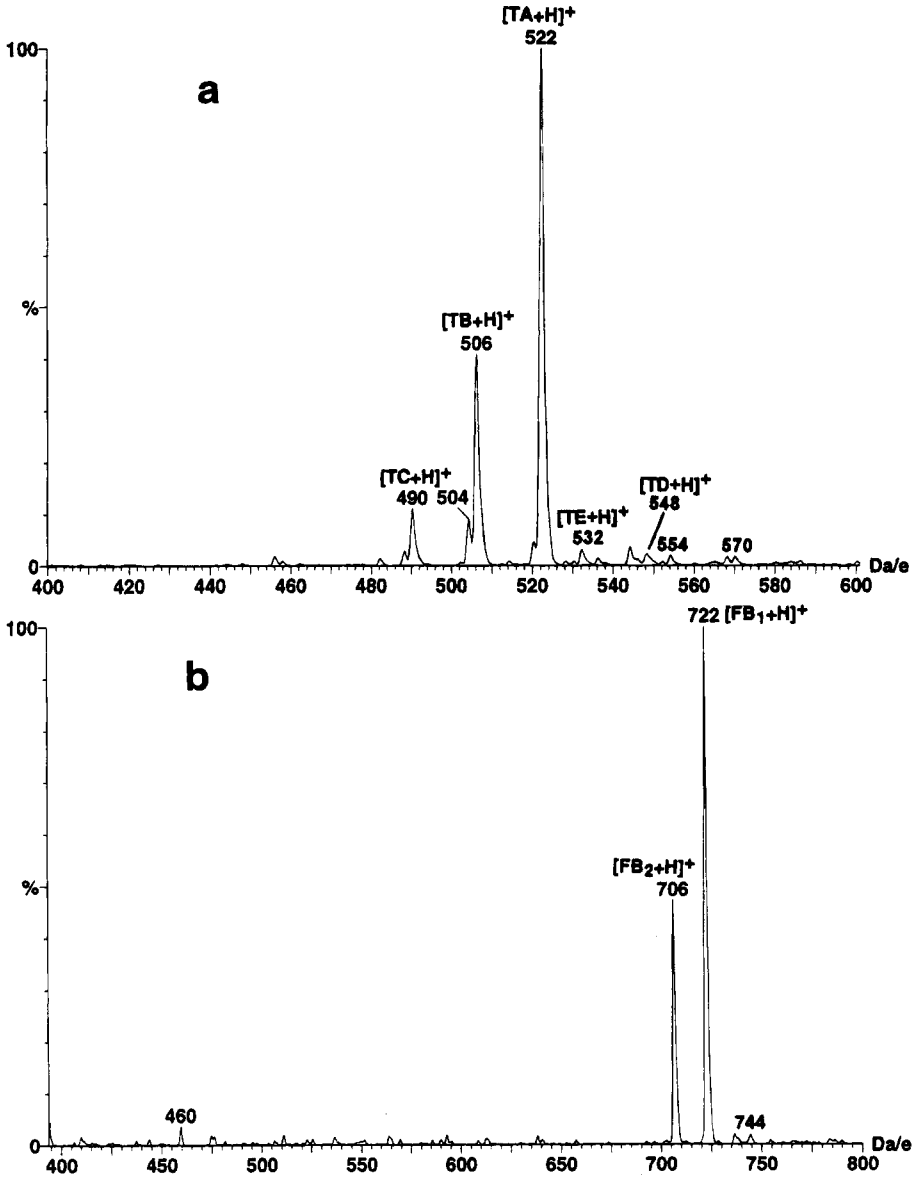

Figure 2. Positive electrospray mass spectra of (a) *A. alternata* liquid culture extract and (b) a mixture of fumonisins FB_1 and FB_2 (approximately 10 ng/μL).

Da/e, respectively, with relatively minor amounts of 744 Da/e $[M + Na]^+$ formed during ionization (Figure 2b).

Unfortunately, the relative yields of sodium adducts of these compounds vary in relation to the concentration of sodium in the sample. This relationship complicates the use of $[M + Na]^+$ as a reliable indicator of the presence of any of the congeners in the absence of a constant sodium concentration. The ratio of $[M + H]^+$ to $[M + Na]^+$ also appeared to depend upon the presence of trace amounts of other basic substances. For example, the presence of NH_3 (observed as NH_4^+ at 18 Da/e) as a contaminant remaining in the transfer line between the injector and the electrospray probe from analysis of other samples containing NH_3 affected the relative abundances of sodium adduct peaks (data not shown). These results highlight the fact that electrospray ionization is a competitive ionization process with the attendant risk that protonation of analytes that have low proton affinities can be suppressed when more basic substances, including the more basic mycotoxins, are present even in trace amounts.

Negative mode ESI spectra of the same preparations of AAL toxins and fumonisins provided spectra with abundant $[M - H]^-$ peaks (Figure 3) but were simpler than the corresponding positive mode spectra due to the absence of peaks resulting from adducts with alkali metal ions. In addition, the relative ionization efficiencies of the acetylated AAL congeners increased in the negative mode compared to the positive mode. Although the negative mode is approximately an order of magnitude less sensitive than positive ionization for the toxins containing a free amino group, the absolute response of the acetylated compounds is enhanced, particularly when other basic substances are present. This improvement in efficiency enabled us to observe a peak at 562 Da/e, which we tentatively attributed as the N-acetylated form of toxin TA. The ability to detect all toxin congeners suggests that the negative ionization is preferable to positive ionization for screening for all known SAMs, and the peak heights in the negative mode are more reliable in reflecting the amounts of the various congeners present.

Negative mode ESI of FB_1 and FB_2 yielded abundant deprotonated ions at 720 and 704 Da/e, plus the doubly charged $[M - 2H]^{2-}$ ions at 360 and 352 Da/e, respectively (Figure 3b). We found appreciable variability in the ratio of intensities of [M –

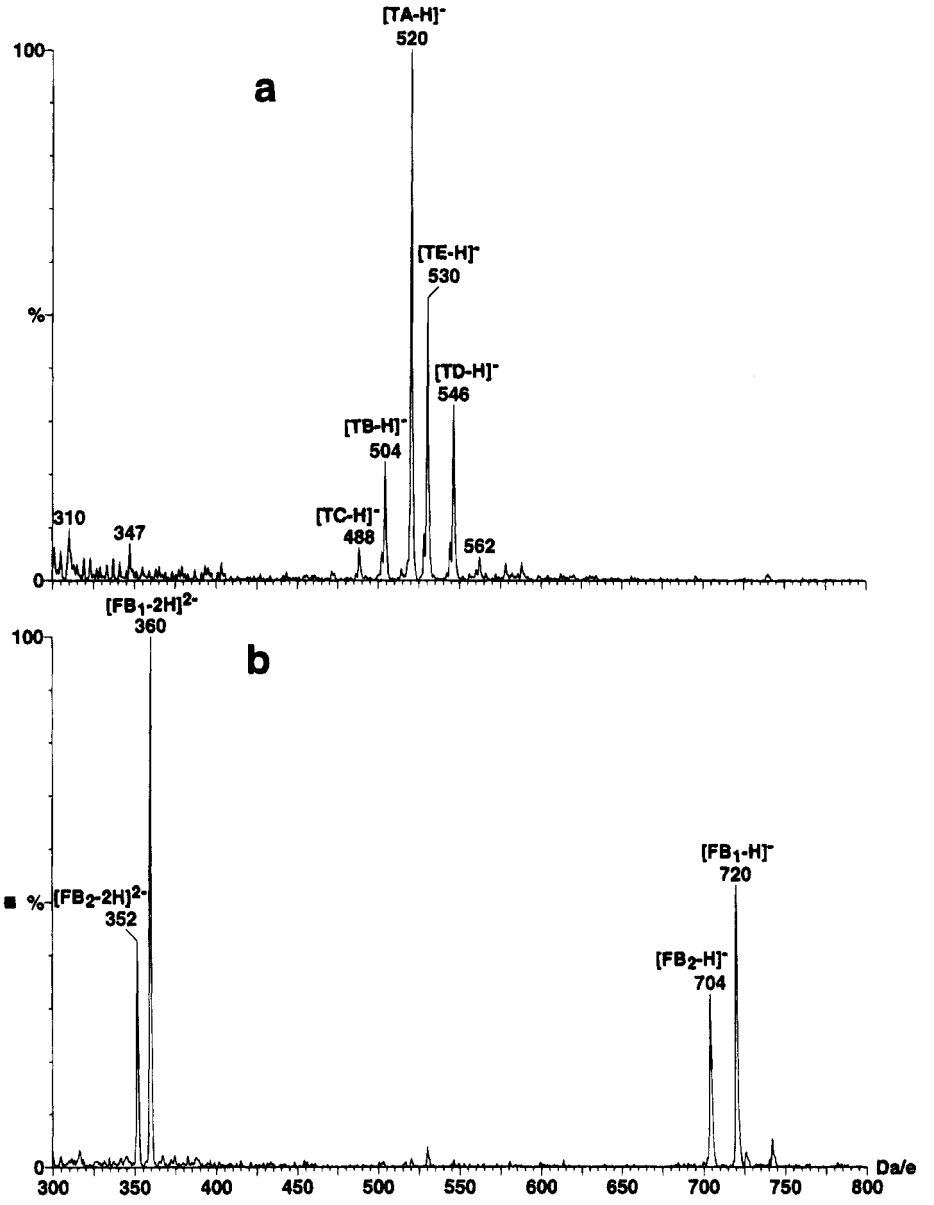

Figure 3. Negative electrospray mass spectra of (a) *A. alternata* liquid culture extract and (b) a mixture of fumonisins FB_1 and FB_2 (approximately 50 ng/μL each).

$H]^-$ to $[M\text{-}2H]^{2-}$ peaks, which ranged from 0.5 to 10 in spectra generated on different days. An earlier report by Siu et al.[39] found that the efficiency of ionization of multiply charged ions increased substantially with decreasing distance between the probe tip and the counter electrode in negative mode ESI. Others factors such as nebulizer gas flow and the presence of contaminants were cited as additional factors potentially confounding the ionization process. In this study, the variability in the distribution of charge states is attributed to variations in pH of the mobile phase. Although the presence of an additional peak can complicate the spectra, the doubly charged ion does serve as additional evidence of the identity of the deprotonated peak. The observation of $[M - 2H]^{2-}$ for the fumonisins but not the AAL toxins can be attributed to greater difficulties in removing a second proton from a single tricarballylic acid group.

Collision Activated Dissociation. (a) Positive Mode. Low-energy CAD was performed in the collision cell at collision potentials that were varied from −5 to −250 V. Although optimum results depend on specific instrumental conditions, we obtained the best results in terms of the limit of detection (LOD) and information content with the cell potential between −15 and −50 V. A common fragmentation pattern was found under these conditions in the daughter ion spectra of $[M + H]^+$ ions for all SAMs. For the AAL toxins, fragmentation of $[M + H]^+$ yielded an abundant daughter ion at $[M+H - TCA]^+$, corresponding to a loss of the tricarballylic acid group (TCA) (Figure 4a and Table 1). The presence of a succession of fragments at $[M + H - TCA - xH_2O]^+$ by dehydration, where x is an integer that ranges from 1 to the number of hydroxyl groups (n) in the molecule, provides valuable structural information indicative of the number of hydroxyls in the molecule. For the acetylated compounds (TD and TE) additional peaks are observed corresponding to $[M + H - TCA - nH_2O - 42]^+$ and $[M + H - TCA - (n - 1)H_2O - 42]^+$, where the loss of 42 Da is attributed to loss of ketene from the N-acetyl group (Figure 4b).

The collision energy required for generation of a spectrum of the daughters of protonated TA (40 eV, Figure 4a) is higher than that required to obtain a daughter spectrum with comparable

(39) Siu, K. W. M.; Gardner, G. J.; Berman, S. S. *Org. Mass Spectrom.* **1989**, *24*, 931–942.

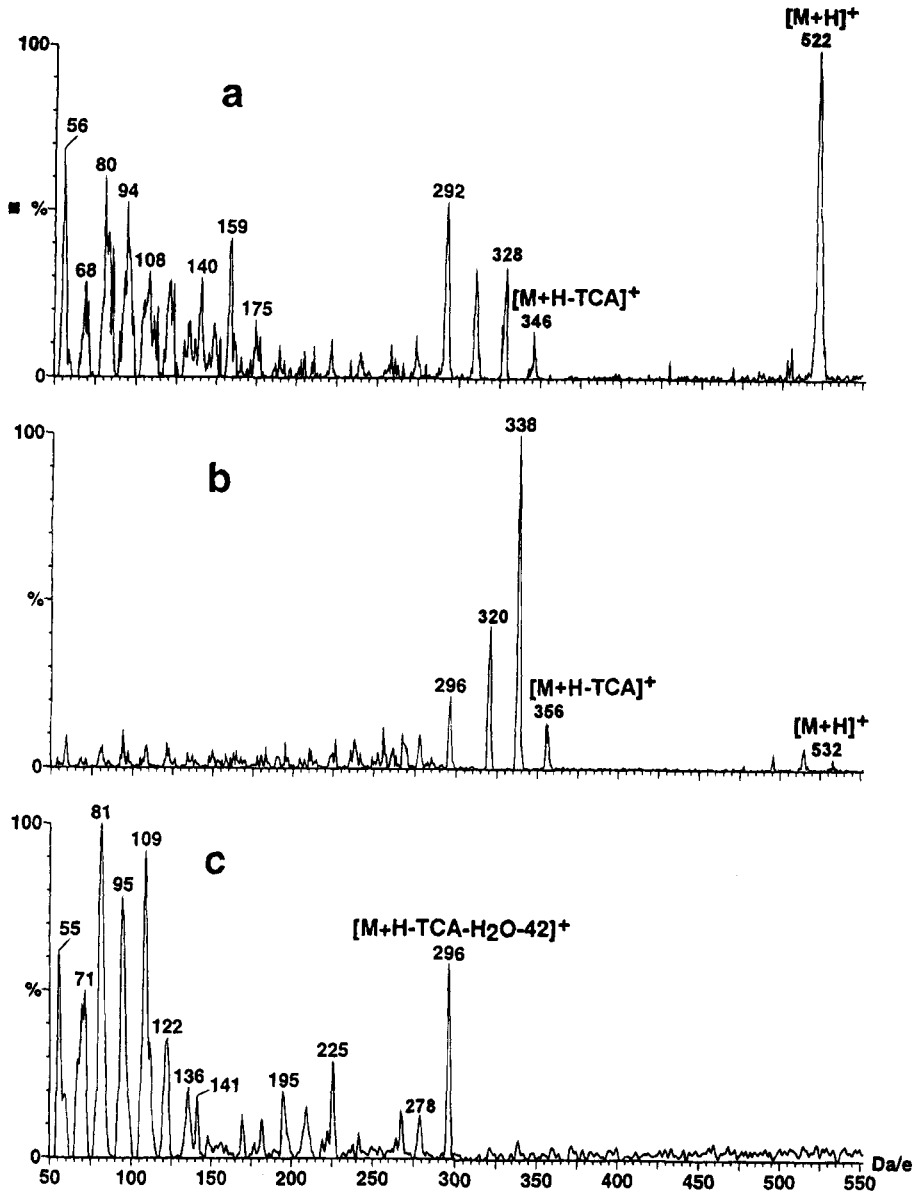

Figure 4. CAD daughter spectra of protonated AAL toxins (a) TA at 40 eV collision energy, (b) TE at 15 eV collision energy, and (c) TE at 40 eV collision energy.

Table 1. Fragment Ions (Da/e values) Observed under Positive Collision Activated Dissociation Conditions

toxin	$[M+H]^+$ parent	$-H_2O$	$-2H_2O$	$-3H_2O$	$-TCA$	$-TCA-H_2O$	$-TCA-H_2O-42$	$-TCA-2H_2O$	$-TCA-2H_2O-42$	$-TCA-3H_2O$	$-TCA-3H_2O-42$	$-TCA-4H_2O$	$-2TCA$	$-2TCA-H_2O$	$-2TCA-2H_2O$	$-2TCA-3H_2O$
TA	522	504	486	468	346	328		310		292		274				
TB	506	488	470	452	330	312		294		276						
TC	490	472	454		314	296		278								
TD	548	530	512	494	372	354		336	294	318	276					
TE	532	514	496		356	338	296	320	278							
AcTA	564	546	528	510	388	370		352	310	334	292					
FB_1	722	704	686	668	546	528		510		492			370	352	334	316
FB_2	706	688	670		530	512		494					354	336	318	

fragmentation for the acetylated toxin TE (Figure 4b). This is also a consequence of the less basic character of the amide, which increases the delocalization of the positive charge and facilitates fragmentation at more sites in the toxin molecule. Daughter spectra of AAL toxins presented here are very similar to spectra from Caldas et al.,[6] who used FAB ionization and high-energy CAD on a magnetic sector instrument. Although the energy per collision (E_{lab}) involved in the FAB experiment (8 keV) is much greater than that in a quadrupole instrument, the current study was conducted with collision gas pressures that yielded multiple collisions with argon, whereas the previous investigation used single collision conditions with helium as collision gas.

The low mass fragments in the SAM daughter spectra are attributed to extensive fragmentation yielding fragments that are indicative only of the hydrocarbon backbone and, consequently, offer little value for confirmation or screening of SAMs. These

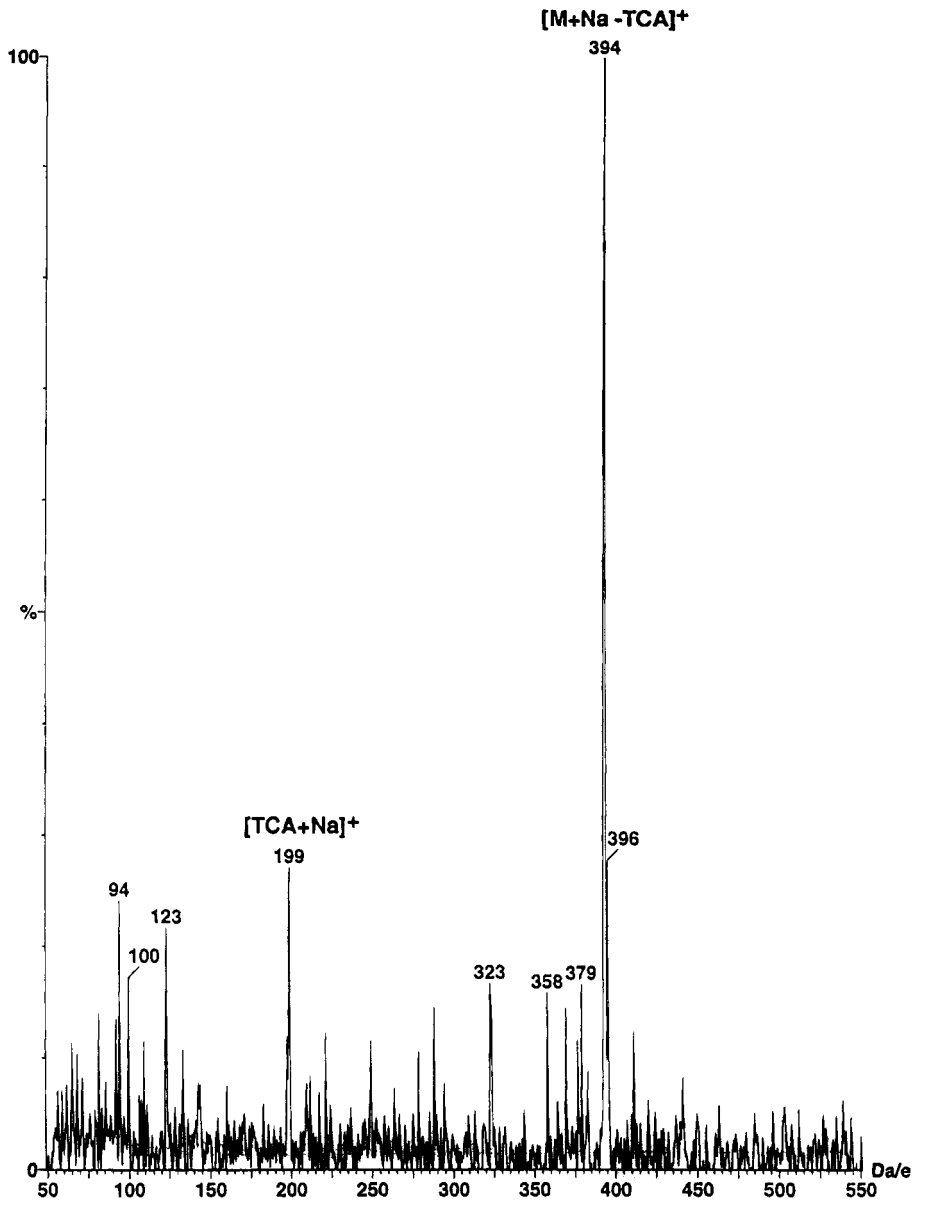

Figure 5. CAD spectrum (40 eV) of daughters of $[M + Na]^+$ from AAL toxin TD.

low mass ions dominate the spectra at higher collision energy (Figure 4c), which is consistent with the results reported by Naylor and Lamb during CAD studies of peptides[40] and those of Schweer and co-workers studying thromboxanes.[41]

As discussed above, the formation of $[M + Na]^+$ represents a major ionization pattern for the acetylated SAMs in positive mode. Generation of daughter spectra of sodium adducts of TD and TE yielded fewer fragments which did not provide additional structural information. At any collision energy applied, the main peaks were attributed to $[M + Na - TCA]^+$ and $[TCA + Na]^+$ (Figure 5). In examining the effect of the Li^+, Na^+, and K^+ ions of ceramides on the CAD fragmentation, Qinghong and Adams found that increasingly competitive release of Cat^+ for the high mass $[M + Na]^+$ significantly reduced the abundance of the structurally informative product ions (e.g., information about the number of hydroxyls).[42] This behavior is a consequence of ion-molecule interaction energies and ligand–Cat^+ bond energies which decrease with increasing ionic radius of the alkali metal ion.[43,44]

Losses of the TCA groups and H_2O dominate the spectra of the daughter ions of $[M + H]^+$ of FB_1 and FB_2 (Figure 6, Table 1). After consecutive losses of two TCA groups, the number of water losses corresponds to the number of hydroxyl groups in the molecule. The spectrum of FB_2 shows that this interpretation likely will hold for other fumonisins, and the FB_1 daughter spectrum presented here is similar to those reported by Chen et al.[22] and Korfmacher et al.,[23] who used ion spray and FAB ionization, respectively. More recently, Plattner and Branham[20] found the same fragmentation pattern using FAB ionization and a quadrupole mass spectrometer.

As a simple alternative to the use of tandem mass spectrometry, CAD spectra in the transport region were obtained by increasing the potential difference between the high-voltage

(40) Naylor, S.; Lamb, J. H. *Rapid Commun. Mass Spectrom.* **1990**, *4*, 251–255.
(41) Schweer, H.; Mackert, G.; Seyberth, H. W. *Biomed. Environ. Mass Spectrom.* **1990**, *19*, 94–96.
(42) Qinghong, A.; Adams, J. *Anal. Chem.* **1993**, *65*, 7–13.
(43) Smith, S. F.; Chandrasekhar, J.; Jorgensen, W. L. *J. Phys. Chem.* **1982**, *86*, 3308–3318.
(44) Eliezer, I.; Krindel, P. *J. Chem. Phys.* **1972**, *57*, 1884–1891.

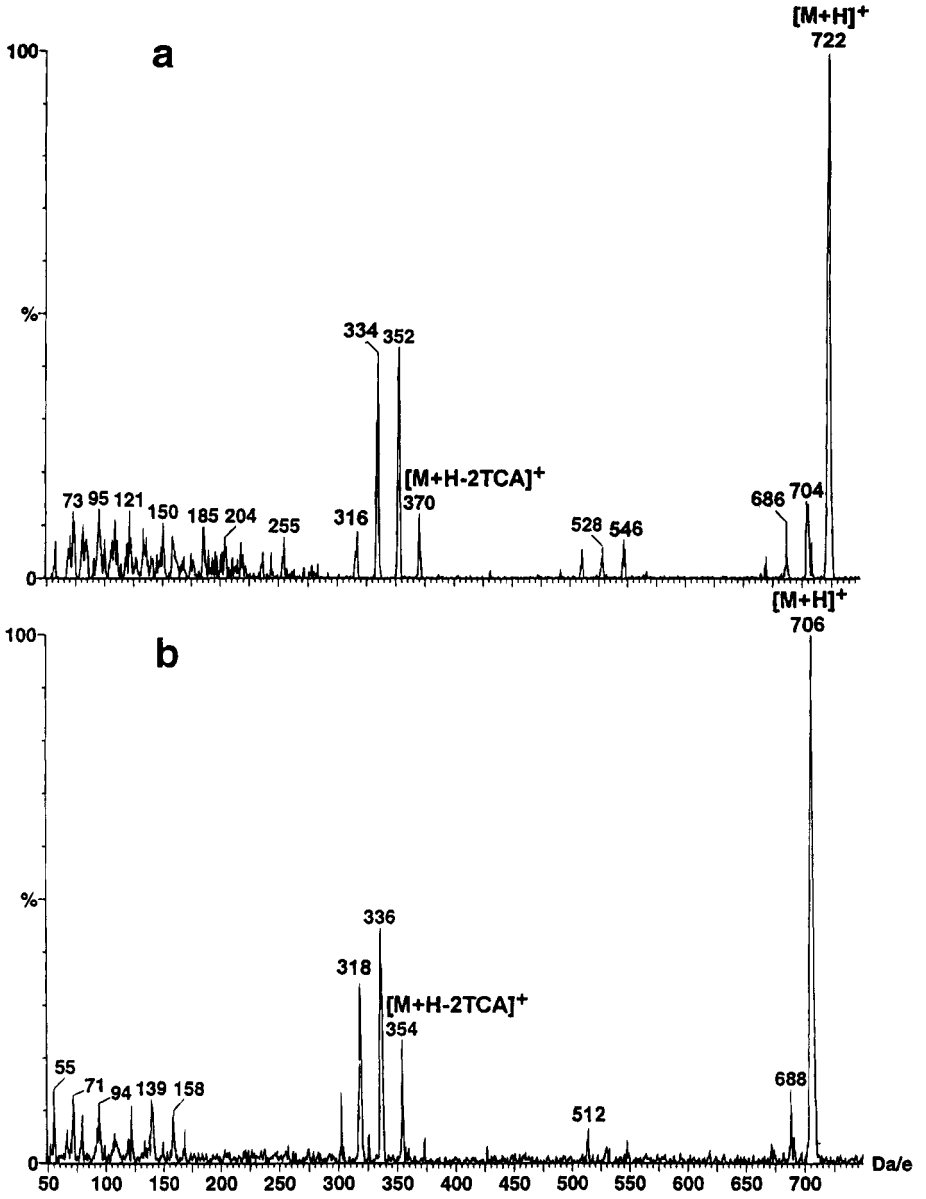

Figure 6. CAD (35 eV collision energy) spectra of daughters of $[M + H]^+$ from fumonisins (a) FB_1 and (b) FB_2.

capillary and the first skimmer (lens 1). At increased potential difference, all ions are accelerated in a region of sufficient pressure (~1 mBar) to result in frequent ion–molecule collisions and collisional activation. This method is very efficient, resulting in 80% or better conversion of a molecular ion to daughter ions and depositing up to 24 eV of internal energy in the molecule.[37] Transport region CAD has been used for studies of multiply charged peptide ions produced by ESI.[45] In the present study, the potential of lens 1 was varied from a voltage where no fragmentation was observed to 150 V. The resulting spectra for TA and FB_1 (Figure 7) showed fragmentation patterns similar to those observed using collision cell CAD of the entire congener set of SAMs tested (Table 1).

Based on these experiments, it appears that structural information for these molecules can be obtained in the absence of a second mass analyzer, although prior chromatographic separation is required as impurities can complicate the spectra in the absence of the ability to isolate the ion of interest. In addition, the ability to produce fragments via transport region CAD allows for confirmation of the presence of SAMs to be performed at low levels using selected ion monitoring of $[M + H]^+$ and abundant fragment ions. Such experiments benefit from the high collision efficiency and avoidance of signal losses which occur due to imperfect fragmentation efficiencies in tandem mass spectrometers.

(b) Negative Mode. At all collision cell potentials studied (10–250 V), the fragmentation pattern in negative daughter spectra of deprotonated SAMs corresponds to the cleavage at the tricarballylic ester bond (Figure 8). Absolute and relative abundances of the peaks, however, change with the energy applied. At lower collision energies, the major fragment for all of the AAL toxins is at 157 Da/e, corresponding to $[TCA - H - H_2O]^-$ (Figure 8a), while FB_1 also yields a peak at $[M - H - 157]^-$ (Figure 8b) which is very sensitive to the energy applied and difficult to detect. As the collision cell potential was increased (>50 V), fragments at 131 ($[TCA - H - CO_2]^-$), 113 ($[TCA - H - H_2O - CO_2]^-$), 87 ($[TCA - H - 2CO_2]^-$) and 69 Da/e ([TCA

(45) Katta, V.; Chowdhury, S. K.; Chait, B. T. *Anal. Chem.* **1991**, *63*, 174–178.

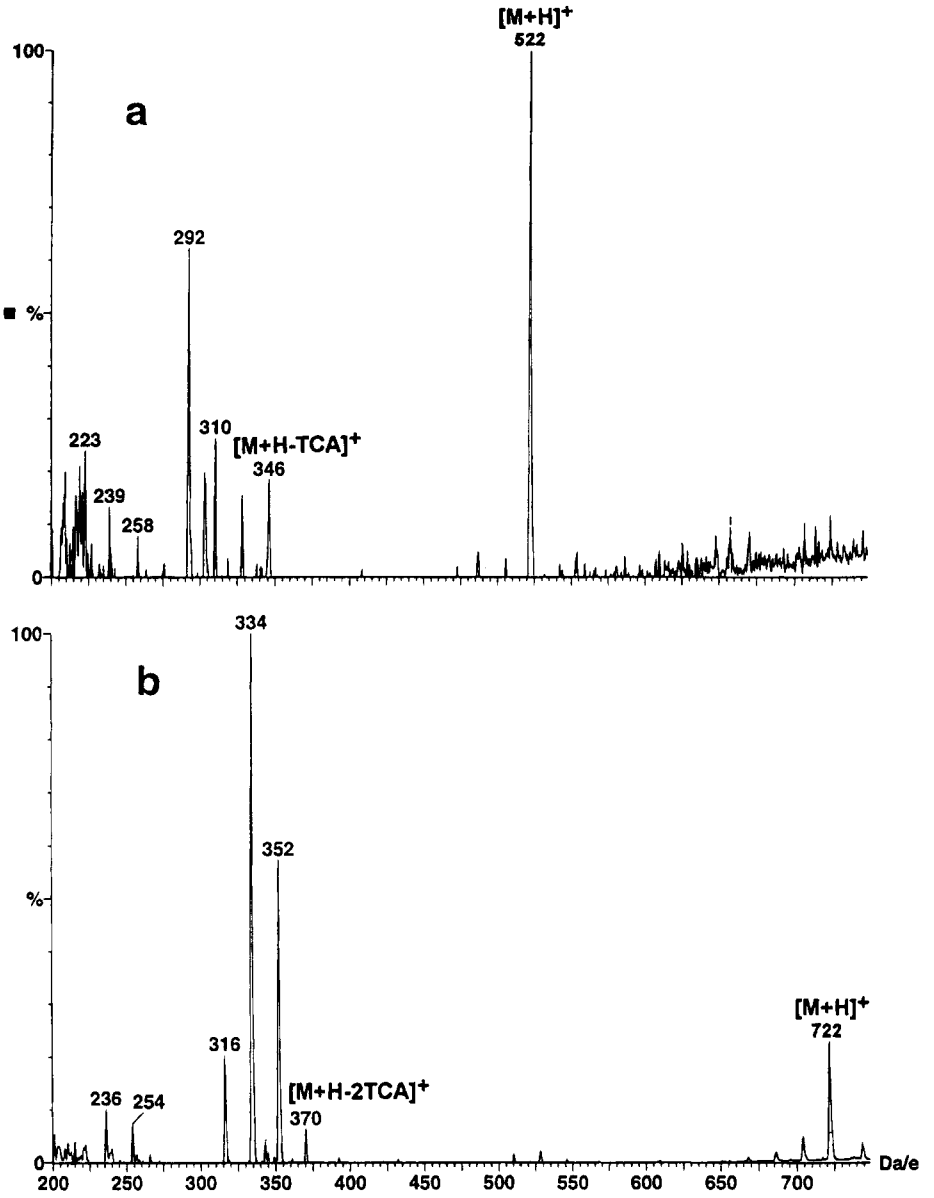

Figure 7. Positive mode electrospray spectrum using source transport region CAD (lens 1 at 120 V) of (a) purified AAL toxin TA and (b) fumonisin FB_1.

$- H - 2H_2O - 2CO_2]^-$) became apparent (Figure 8c). At a cell potential of 250 V, the peak at 69 Da/e predominated. Negative CAD in the transport region yields fragmentation patterns similar to those generated by CAD in the collision cell (results not shown).

Identical fragments were seen in a spectrum of the daughters of deprotonated tricarballylic acid (Figure 9). Interpretation of this fragmentation was facilitated by comparison with the daughter spectrum of β-methyltricarballylic acid. In contrast to the singly charged molecule, the daughter spectrum of the doubly deprotonated FB_1, obtained at a collision cell potential of 20 V, showed more extensive fragments from the tricarballylic acid moiety, suggesting the more extensive release of energy from fragmentation of doubly charged ions (Figure 10).

Acetylated TA. Previously, no evidence of the acetylated analog of AAL toxin TA (AcTA) was found when samples were analyzed by positive FAB/MS.[6] However, in the present study, a CAD daughter spectrum generated for the minor peak at 562 Da/e observed in negative ESI mode for the *A. alternata* f.sp. *lycopersici* culture filtrate exhibited peaks at 157, 113, 131, and 69 Da/e characteristic of the tricarballylic acid group. The 562 Da/e peak appeared in extracts regardless of whether or not the preparation had been exposed to acetic acid during purification. We conclude that the peak is the acetylated analog of AAL toxin TA and not an unrelated contaminant.

Chromatographic evidence of the presence of this new toxin was obtained during the HPLC purification of a TD fraction obtained by flash chromatography. An HPLC peak eluting before TD was detected absorbing at 210 nm and gave strong peaks at 562 Da/e in negative ESI and 564 Da/e in positive ESI mass spectra. Positive daughter spectra of the 564 peak showed fragmentation similar to the acetylated AAL toxins TD and TE, demonstrating fragments corresponding to combined losses of TCA, H_2O, and 42 Da (Table 1). The ^1H NMR spectrum of this fraction showed a peak at 1.95 ppm, corresponding to the methyl protons of the N-acetyl group. The COSY spectrum showed coupling of the two characteristic pairs of peaks corresponding to the protons H_{13} and H_{14}, one pair corresponding to the isomer that has TCA esterified at C_{13} and the other at C_{14}.[4,6] Also, the coupling pattern of the hydrogens at C_1 to C_6 confirmed the

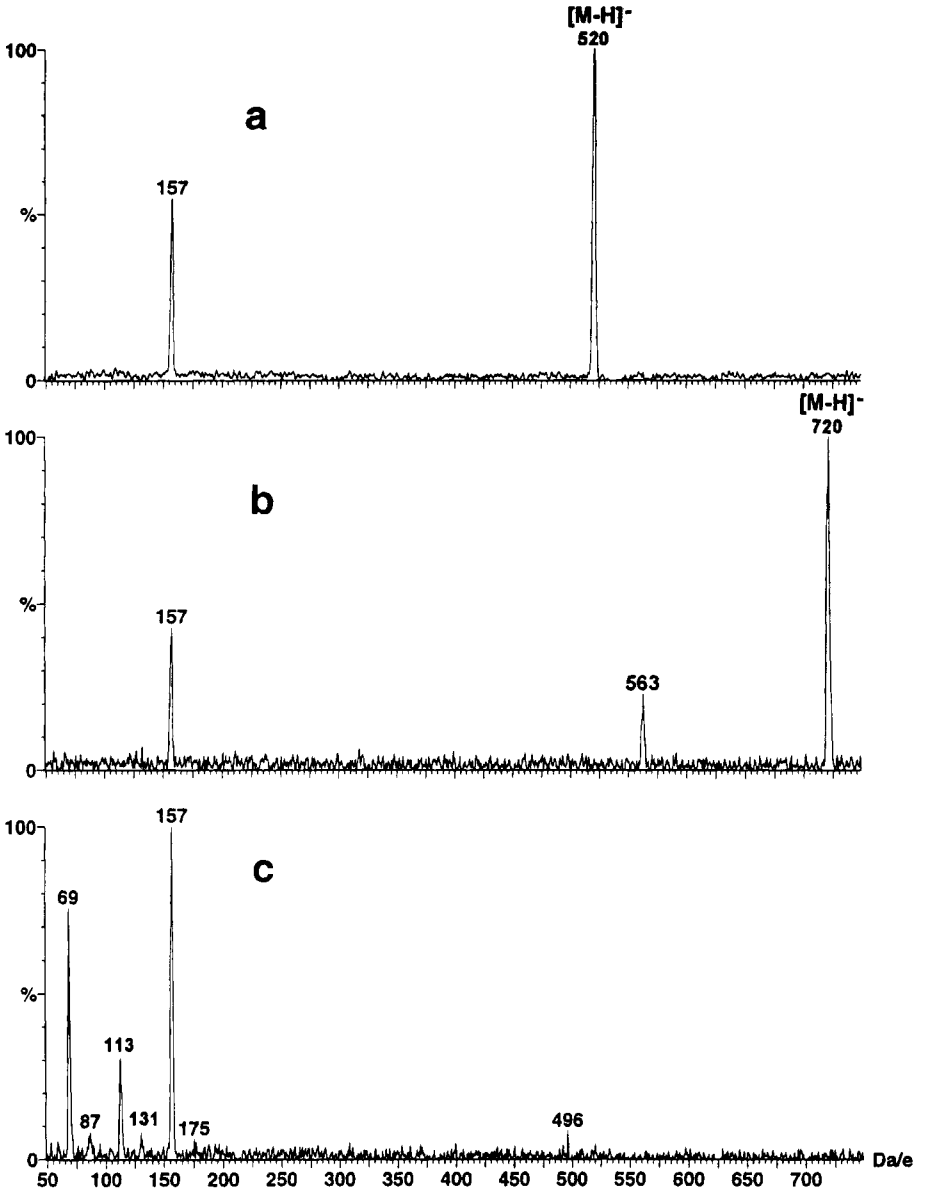

Figure 8. CAD spectra of daughters of $[M - H]^-$ from (a) AAL toxin TA (20 eV), (b) FB_1 (20 eV), and (c) AAL toxin TA at 50 eV collision energy.

position of the hydroxyl groups in the molecule (Table 2). It is curious, from the biosynthetic point of view, that this congener is the one which is present in the lowest concentration of the acetylated congeners, while its counterpart TA is the most abundant of all AAL toxins produced in culture.

Detection of SAMs in Food Matrices. Experiments were conducted in duplicate to determine the relative merits of using positive and negative ESI in SIM mode to detect SAMs in food matrices. Measurement of the peak area was used as a basis of quantification. In positive mode, the LOD of standard FB_1 solution (signal-to-noise ratio of 5:1) was 0.2 μg/mL injected, and the response was linear over the range of 0.2–20 μg/mL. When corn extracts that had been spiked with FB_1 were analyzed, the LOD rose to 10 μg/mL injected, which corresponds to 20 μg/g corn. Evaporation of the corn extract to one-fifth its original volume failed to improve the sensitivity. These results indicate that the response to FB_1 in ESI is matrix dependent, as other components in the sample compete with and suppress ionization of the analyte of interest. Based on the concentration of FB_1 reported in various corn-based foods (0.02–40 μg/g),[17,21,46] the use of ESI for analysis of fumonisins in food products will require more extensive or more specific cleanup than currently used for the analysis of FB_1 by other methods.

Conversely, concentrations of AAL toxins in foodstuffs have yet to be established. However, based upon their chemical and toxicological similarities to fumonisins, the AAL toxins are expected to exert effects on health similar to the effects of fumonisins should they occur in foods at biologically active concentrations. Techniques are not readily available for detection of the N-acetylated forms of AAL toxins.

In the ESI positive mode, the LOD of TA in a standard mixture of TA and TD was 0.4 μg/mL injected compared with the TD signal ($[M + H]^+$), which was smaller by a factor of 2. The lesser sensitivity of TD is attributed to the formation of the sodium adduct at 570 Da/e and fragmentation to give a peak at 530 Da/e corresponding to $[M + H - H_2O]^+$. The LOD of TA in the vegetable juice extract was 10-fold lower (4 μg/mL sample

(46) Pestka, J. J.; Azcona-Olivera, J. I.; Plattner, R. D.; Minervini, F.; Doko, M. B.; Visconti, A. *J. Food Prot.* **1994**, *57*, 169–172.

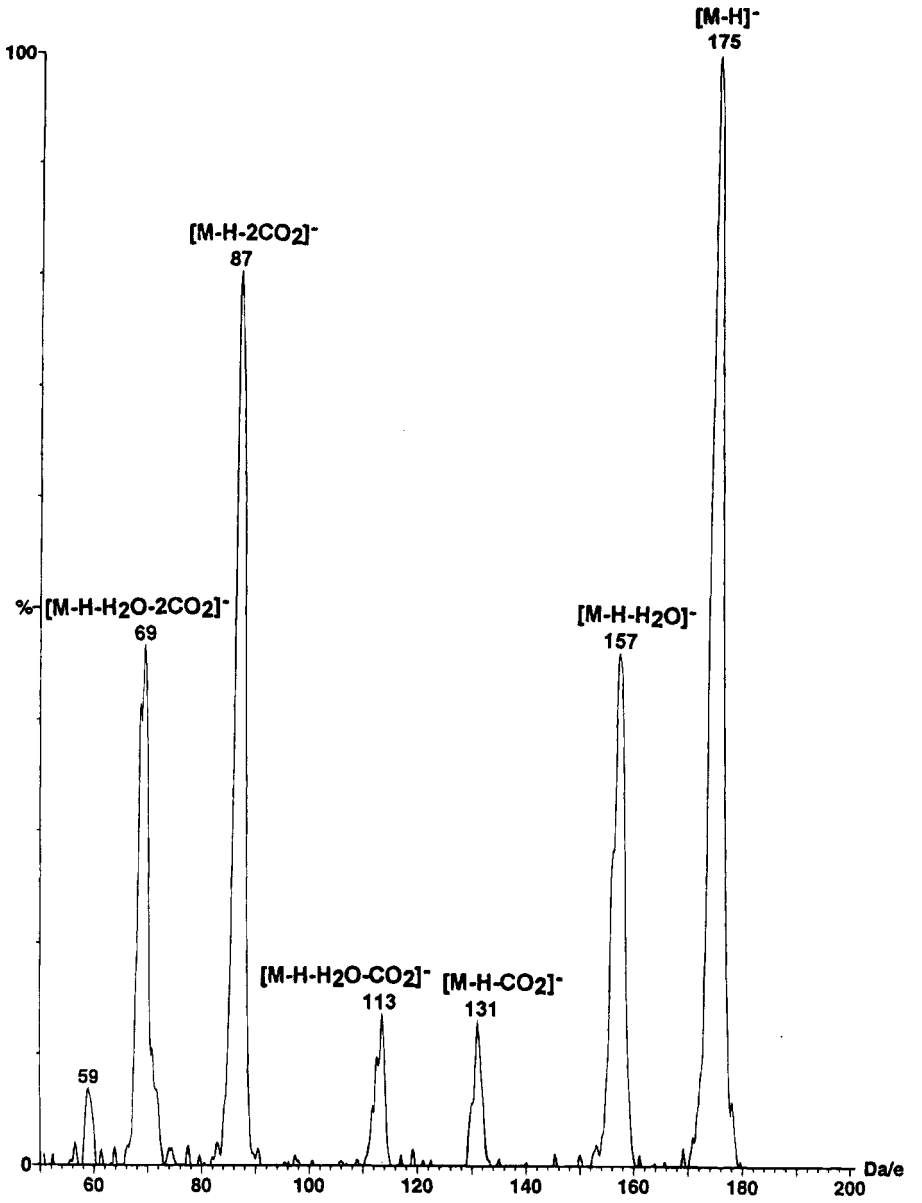

Figure 9. CAD spectrum of daughters of $[M - H]^-$ from tricarballylic acid (100 ng/μL).

Table 2. ^{1}H NMR Chemical Shifts for Acetylated TA Toxin[a]

	δ		δ
H_1	3.27	H_6	1.34
H_1'	3.16	H_{12}	1.63,[d] 1.46[e]
H_2	3.88[b]	$H_{12'}$	1.59,[d] 1.30[e]
H_3	1.59	H_{13}	5.10,[d] 3.77[e,f]
$H_{3'}$	1.47	H_{14}	3.36,[d] 4.77[eg]
H_4	3.65[c]	H_{15}	1.36,[d] 1.76[e]
H_5	3.41		

[a] Chemical shifts were obtained from COSY experiment. [b] m (J = 2.3–2.4 Hz). [c] m (J = 2.0–2.8 Hz). [d] Isomer which has the TCA ester at C_{13}. [e] Isomer which has the TCA ester at C_{14}. [f] m (J = 2.2–3.2 Hz). [g] t (J = 5.9 Hz).

injected) than that for the standard solution, while detection of the TD peaks at 548 ($[M + H]^+$) and 570 Da/e ($[M + Na]^+$) yielded a signal-to-noise ratio of 2:1. Hence, suppression of ionization by the juice matrix was similar for TA and TD. However, the suppression was less intense for either AAL toxin congener in vegetable juice than for FB_1 in the corn extract. As was the case for the corn extract, concentration of the vegetable juice extract to one-fifth its original volume did not improve the LOD.

Negative mode ESI analysis of a standard solution showed that TA LOD (2 μg/ml injected) was half that of TD (1 μg/mL injected). In extracts of vegetable juice, TD had a LOD of 4 μg/mL sample (4 μg/mL injected), and at this level, TA gave a signal-to-noise ratio of 3:1. These results show that the cleanup procedure applied to vegetable juice was more efficient in eliminating the matrix suppression in negative mode than in positive mode for both SAMs.

CONCLUSIONS

Though detection of all known congeners of fumonisins and AAL toxins can be obtained using either positive or negative ESI, negative mode offers clear advantages over positive mode for analysis of SAMs. Negative mode ionization is less likely to be complicated by alkali metal cationization, which is a common phenomenon in analysis of biological samples. Formation of [M

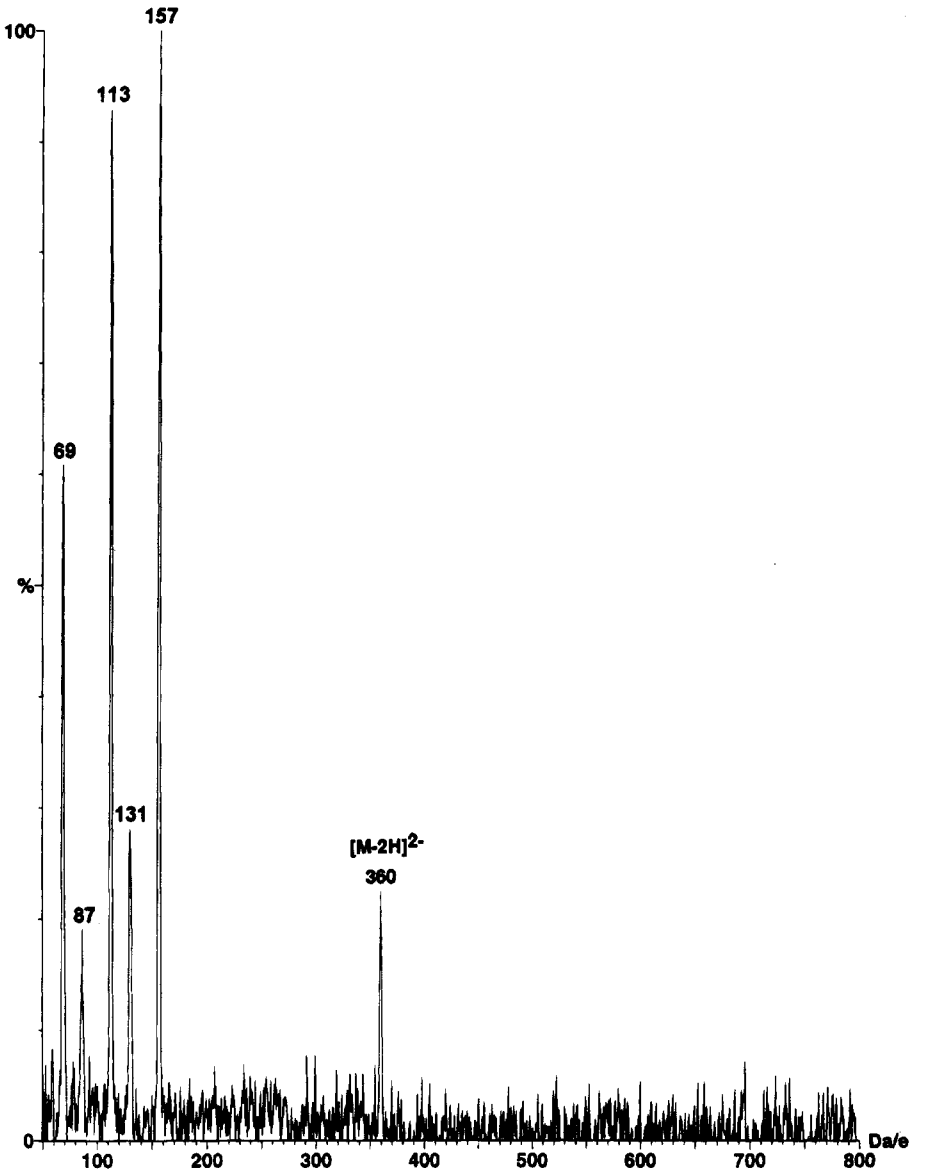

Figure 10. CAD spectrum of daughters of doubly deprotonated FB_1 at 20 V collision cell potential.

$-H]^-$ ions is thus more reliable than formation of protonated molecules, and this is particularly true for N-acetylated SAMs, for which $[M + H]^+$ is often weak or not detectable when more basic substances are present. Aside from the issue of cationization, matrix effects are comparable in negative and positive ion modes. Fragmentation is simpler in negative mode, yielding a smaller number of fragments, all of which are characteristic of the tricarballylic acid group. Overall, these factors make negative ESI analysis attractive for screening and confirmation of SAMs, whereas positive mode ESI is more useful for detailed structural characterization. It is recommended that the two ionization modes and CAD analyses, either in the source region or in collision cells, be used as complementary tools for the analysis of SAMs.

ACKNOWLEDGMENT

Acquisition of the Quattro-BQ mass spectrometer was supported in part by the NIEHS Superfund Basic Research Program (Grant ES-04699) and the NIEHS Center for Environmental Health Science at UC Davis (Grant ES-05707). The Ω-500 NMR spectrometer was purchased in part using NIH Grant 1S10-RR04795 and NSF Grant BBS88-04739 funds. E.D.C. was supported by a CNPq Fellowship from the Brazilian government. This work was presented in part at the 42nd Annual Conference on Mass Spectrometry, Chicago, IL, May 29–June 3, 1994.

Received for review May 27, 1994. Accepted October 3, 1994.[⊗]

AC940545+

[⊗] Abstract published in *Advance ACS Abstracts,* November 1, 1994.